

# INFLUENCE OF HEAT TREATMENT ON THE *IN VITRO* BIOACTIVITY OF ALKALI-TREATED TITANIUM SURFACES

MATTHIEU RAVELINGIEN\*, \*\*, STEVEN MULLENS\*, JAN LUYTEN\*, VERA MEYNEN\*, \*\*\*,  
EVI VINCK\*, \*\*\*\*, CHRIS VERVAET\*\*, JEAN PAUL REMON\*\*

\*Materials Technology, VITO NV (Flemish Institute for Technological Research),  
Boeretang 200, 2400 Mol, Belgium

\*\*Laboratory of Pharmaceutical Technology, Department of Pharmaceutics, Ghent University,  
Harelbekestraat 72, 9000 Ghent, Belgium

\*\*\*Laboratory of Adsorption and Catalysis, Department of Chemistry, University of Antwerp,  
Universiteitsplein 1, 2610 Wilrijk, Belgium

\*\*\*\*SIBAC (Spectroscopy in Biophysics and Catalysis), Department of Physics, University of Antwerp,  
Universiteitsplein 1, 2610 Wilrijk, Belgium

E-mail: matthieu.ravelingien@vito.be

Submitted December 8, 2010; accepted May 28, 2010

## Keywords: ???

*Alkali- and heat-treated titanium surfaces have earlier shown bioactivity. However, sufficient attention has to be paid to the sensitivity of porous titanium substrates to oxidation and nitriding during heat treatment under air. Therefore, in the present study, alkali-treated titanium samples were heat-treated under air, argon flow or vacuum. They were extensively characterized by contact angle measurements, diffuse reflectance infrared Fourier transform (DRIFT) spectroscopy, field emission scanning electron microscopy (FESEM), thin film X-ray diffraction (TF-XRD), Raman spectroscopy, X-ray photoelectron spectroscopy (XPS) and glow discharge optical emission spectroscopy (GDOES). The in vitro bioactivity was evaluated in simulated body fluid (SBF). All heat treatments under various atmospheres turned out to be detrimental for apatite deposition. They led to the thermal decomposition of the dense sodium titanate basis near the interface with the titanium substrate into atmosphere-depending forms of  $Ti_2O_3$  and sublimated  $Na_2O$ . Consequently, less exchangeable sodium ions remained available. This points to the importance of the ion exchange capacity of the sodium titanate layer for in vitro bioactivity.*

## INTRODUCTION

The alkali and heat treatment of titanium surfaces, as firstly described by Kim et al. [1], successfully demonstrated to induce bioactivity both *in vitro* [2-5] and *in vivo* [6-9]. Nevertheless, adverse effects of the heat treatment on the *in vitro* bioactivity have been reported as well [10-13]. Still, it remains indistinct what mechanism is predominant in inhibiting the calcium phosphate deposition. Kim et al. described the dehydration of the gel layer at 400-500 °C and the conversion into an amorphous sodium titanate layer, the densification at 600 °C and the transformation into crystalline sodium titanate and rutile above 700 °C. The exchange rate of  $Na^+$  ions for  $H_3O^+$  ions, and consequently the rates of TiOH formation, reaction with  $Ca^{2+}$  ions and apatite deposition, decreased with the structural change from gel to amorphous and eventually crystalline phase [10].

Chen et al. reported that heat treatment at 600°C in air transformed the sodium titanate hydrogel into an amorphous dehydrated sodium titanate layer containing

small amounts of crystalline rutile, which resisted the formation of TiOH groups during immersion in SBF [11]. Wei et al. observed a decreased apatite-inducing ability of alkali-treated microarc oxidized  $TiO_2$ -based films containing Ca and P after heat treatment at 400 and 600°C. The dehydration at these temperatures was believed to inhibit the  $Ca^{2+}$  ion release and consequently the formation of TiOH groups [12]. Becker et al. reported the decomposition of sodium trititanate during heat treatment at 1050°C and a sodium content decrease due to the sublimation of  $Na_2O$  (Equation 1). Consequently, less sodium ions were available for ion exchange and calcium phosphate deposition was reduced [13].



In the present study, alkali-treated titanium samples were heat-treated under air, argon flow or vacuum because sufficient attention has to be paid to the sensitivity of porous titanium substrates to oxidation and nitriding during heat treatment under air. The microstructure and composition of their surfaces were extensively

characterized and the influence of heat treatment under various atmospheres on the *in vitro* bioactivity was evaluated in SBF.

## MATERIALS AND METHODS

### Alkali and heat treatment

Commercially pure titanium plates (10×10×0.6 mm) are abraded with 1000 grit SiC paper and ultrasonically cleaned in acetone, ethanol and distilled water for 10 min at each step. Subsequently, they are immersed in 5 M NaOH solution for 24 h at 60°C and washed with distilled water. Finally, heat treatments are performed under different conditions: in 10<sup>-6</sup> atm vacuum to 400°C (VAC 400) or 600°C (VAC 600), in 260 l/h argon flow to 600°C (ARG 600) or in air to 600°C (AIR 600) at a rate of 3°C/min. Heating is maintained at 400 or 600°C for 1 h, followed by cooling to room temperature at a rate of 3°C/min.

### Characterization

Cross sections are prepared by a cross section polisher (SM-09010, JEOL, Japan), with an argon ion acceleration voltage of 6 kV and an etching time of 4 h. A 200 nm gold coating on the surface distinguishes substrate from redeposition, which is inherent to the cross section polishing technique. The surface and cross section morphologies are visualized by field emission scanning electron microscopy (FESEM; JSM-6304F, JEOL, Japan), with an operation voltage of 5 kV. The surface phases are identified by thin film X-ray diffraction (TFXRD; X'pert, Philips, The Netherlands) using a Cu-K<sub>α</sub> X-ray source (λ = 1.54056 Å) with a grazing incidence angle of 0.5° and a step rate of 0.01°/s. Resonance-Raman measurements are carried out on a 80-cm Dilor XY-800 Raman scattering spectrometer. The excitation source is a Kr-ion laser (Spectra Physics 2020) at 514.5 nm with a power of 0.8 W. The Raman shift is measured in the range from 200 to 1000 cm<sup>-1</sup>. The depth profile is analysed by glow discharge optical emission spectroscopy (GDOES), sputtering in an argon atmosphere and detecting the elements Ti (365 nm), O (130 nm) and Na (590 nm).

### *In vitro* bioactivity

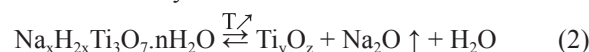
The simulated body fluid (SBF) is prepared as described by Kokubo & Takadama [14]. The *in vitro* bioactivity is evaluated by immersing the samples in triplicate in 50 mL SBF at 37°C for 7 days. After gently washing with distilled water and drying during 24 h at 40 °C in air, the samples are analysed gravimetrically. The deposited coating is visualized by FESEM and the calcium phosphate phase is identified by TFXRD.

## RESULTS AND DISCUSSION

After heat treatment, the TF-XRD diffractograms and Raman spectra showed a decrease of the sodium titanate peak intensities, according to the sequence NaOH + AIR 600 > NaOH + ARG 600 ≈ NaOH + VAC 400 > NaOH + VAC 600 (Figures 1 and 2). The decomposition of sodium titanate coexisted with the formation of atmosphere-depending forms of Ti<sub>y</sub>O<sub>z</sub>. Rutile was formed after 600°C in air (Figure 1 and 2) and the reducing vacuum environment enabled the formation of the suboxide TiO after 600°C in vacuum (Figure 1). The appearance of the oxygen deficient Ti<sub>6</sub>O could be attributed to oxygen diffusion in the titanium substrate (Figure 1) [15]. Possibly other forms of Ti<sub>y</sub>O<sub>z</sub> were formed but could not be detected by TFXRD or Raman, due to their amorphous state.

Kim et al. identified the titanate layer on titanium after alkali oxidation and heat treatment in air as being sodium pentatitanate (Na<sub>2</sub>Ti<sub>5</sub>O<sub>11</sub>) [1,10]. However, Glasser and Marr reported earlier that the JCPDS card 11-289 corresponds to a mixture of Na<sub>2</sub>Ti<sub>3</sub>O<sub>7</sub> and Na<sub>2</sub>Ti<sub>6</sub>O<sub>13</sub> instead of Na<sub>2</sub>Ti<sub>5</sub>O<sub>11</sub> [16]. The TFXRD diffractogram (Figure 1) and the Raman spectrum (Figure 2) of the alkali-treated sample showed a remarkable similarity with those of titanate nanostructures [17-19]. Kasuga et al. firstly reported the production of titania nanotubes after hydrothermal alkali treatment of TiO<sub>2</sub> [20]. The formation mechanism and the effect of sodium removal on the thermal stability of these nanostructured titanates has been studied by Morgado et al. [21]. Nanostructured sodium trititanates, with general formula Na<sub>x</sub>H<sub>2x</sub>Ti<sub>3</sub>O<sub>7</sub>·nH<sub>2</sub>O, were formed after hydrothermal alkali treatment of anatase powder. Based on the TFXRD and Raman results, it is believed that the sodium titanate hydrogel layer of the alkali-treated sample corresponds to the trititanate crystal structure with general formula Na<sub>x</sub>H<sub>2x</sub>Ti<sub>3</sub>O<sub>7</sub>·nH<sub>2</sub>O.

The GDOES depth profiles showed that the sodium titanate decomposition after 400°C in vacuum and after 600 °C in air or argon was accompanied by a sodium shift towards the sample surface (Figure 3). The sodium signal from the GDOES depth profile disappeared completely after 600°C in vacuum. The TF-XRD diffractogram and Raman spectrum of the sample treated at 600°C in vacuum showed the complete decomposition of sodium titanate (Figures 1 and 2). These findings indicate that the decomposition of the sodium titanate coexists with the depletion of sodium. The sodium release can be explained by the sublimation of Na<sub>2</sub>O (Equation 2). During treatment at 600°C in vacuum, Na<sub>2</sub>O is removed from the environment by the vacuum and the equilibrium of the reaction completely shifts to the right, which is consistent with Le Chatelier's principle. Therefore, the main reaction of the thermal decomposition of the sodium titanate layer can be described as follows:



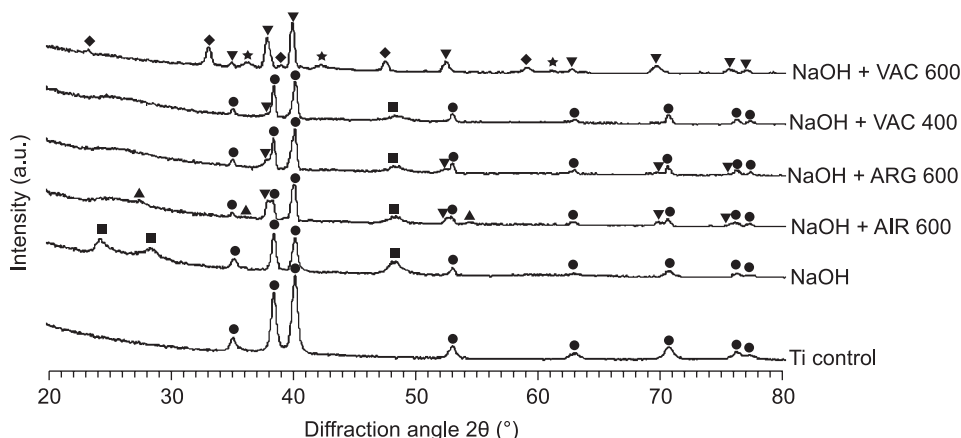


Figure 1. TF-XRD diffractograms of alkali- and heat-treated surfaces.

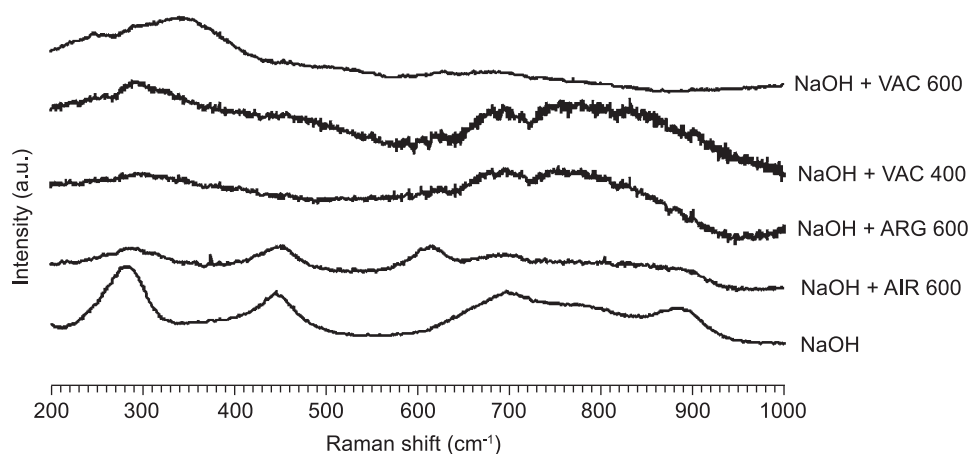


Figure 2. Raman spectra of alkali- and heat-treated surfaces.

 Table 1. Overview of alkali and heat treatment characterization and *in vitro* bioactivity.

	$\text{Na}_x\text{H}_{2-x}\text{Ti}_3\text{O}_7 \cdot n\text{H}_2\text{O}$ (TF-XRD)	$\text{Ti}_6\text{O}$ (TF-XRD)	$\text{Na}_x\text{H}_{2-x}\text{Ti}_3\text{O}_7 \cdot n\text{H}_2\text{O}$ (Raman)	sodium in depth profile (GDOES)	cross section fibrous layer morphology (FESEM)	<i>in vitro</i> bioactivity
Ti control	-	-	/	+	no layer	-
NaOH	+++	-	+++	+++	dense basis	+++
NaOH + AIR 600	+	++	+	+++	porous basis	-
NaOH + ARG 600	+	+	+	+++	porous basis	-
NaOH + VAC 400	+	+	+	+++	porous basis	-
NaOH + VAC 600	-	+++	-	-	porous basis	-
					/	not measured
					-	no detection
					+	weak detection
					++	medium detection
					+++	intense detection

The alkali-treated sample shows a mass increase of  $1.34 \pm 0.07 \text{ mg/cm}^2$  and is completely covered by globules after 7 days of immersion in SBF, while all other samples do not show any precipitation after gravimetric and FESEM analysis (Figure 4). The TF-XRD diffractogram of the alkali-treated sample

identifies the precipitated globules as hydroxyapatite and no hydroxyapatite diffraction peaks are observed for the heat-treated samples (data not shown).

The dense structure at the basis of the sodium titanate layer on the alkali-treated sample, near the interface with the titanium substrate and visualized by cross section

FESEM analysis (Figure 5), disappears after all heat treatments and can be correlated with (Table 1):

- the sodium signal in the GDOES depth profile, which also reaches its maximum near the interface with the titanium substrate (Figure 3);
- the sodium titanate detected by TF-XRD and Raman, which also decomposes to a certain extent after all heat treatments (Figures 1 and 2).

Correlated with the *in vitro* bioactivity results (Fig. 4), this indicates that the decomposition of the dense sodium titanate basis near the interface with the titanium substrate, negatively influenced the hydroxy-

apatite deposition. Depending on the sodium content, titanates exhibit different structures. Papp et al. described the layered structure of trititanates, which allowed ion exchange, while at lower sodium contents the tunnel structure of hexatitanates hampered ion exchange [22]. Jonášová et al. demonstrated that sodium removal by water treatment did not reduce the bioactivity [23]. Takemoto et al. showed that sodium removal by dilute HCl between alkali and heat treatment enhanced the calcium phosphate deposition [24]. These findings indicate that the availability of sodium for ion exchange determines the ability to form Ti-OH groups

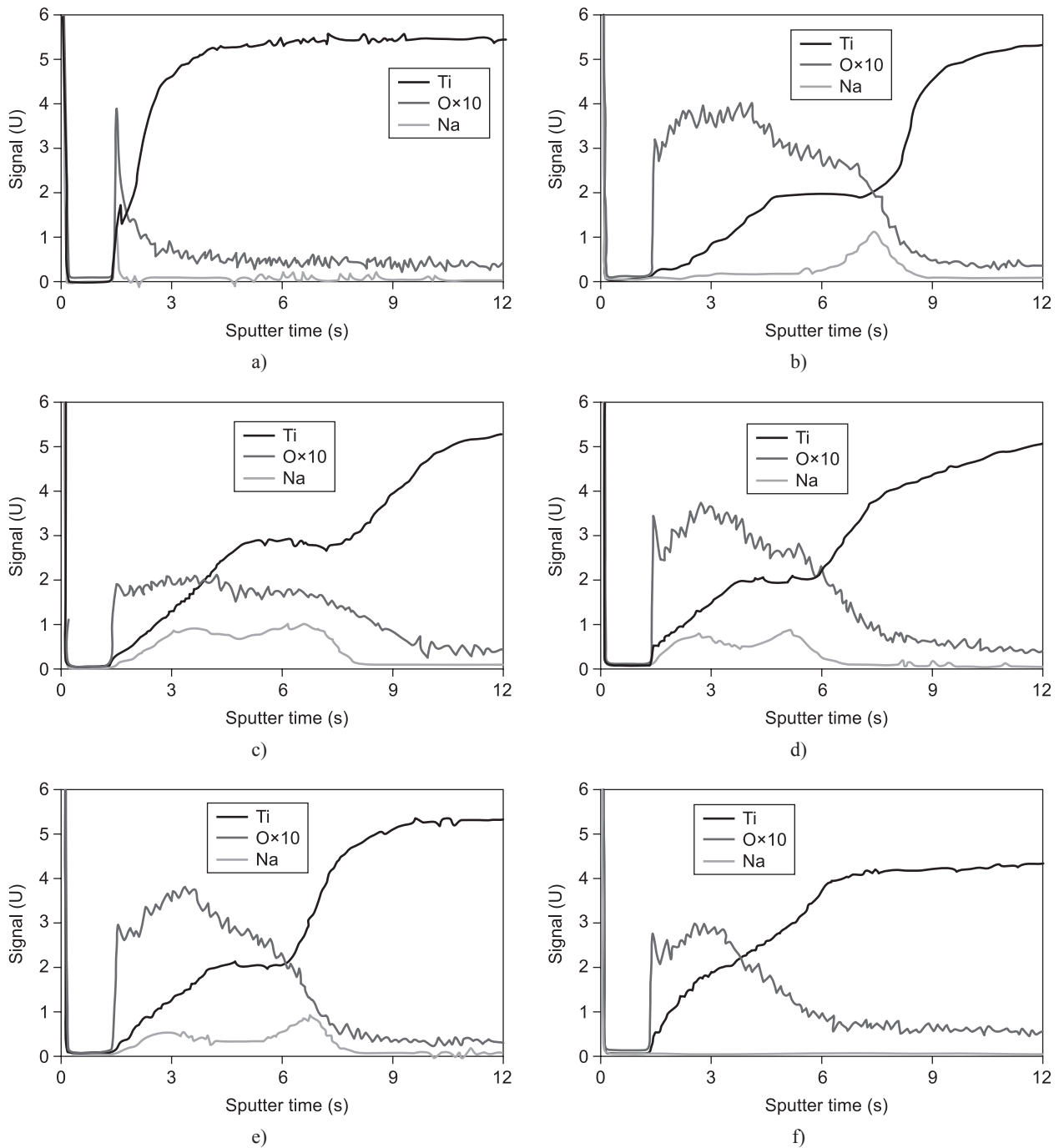


Figure 3. GDOES depth profiles of alkali- and heat-treated samples.

and to deposit apatite. In the present study, the thermal decomposition of sodium titanate into  $Ti_yO_z$  caused a decrease in availability of  $Na^+$  ions. Therefore, less ion exchange with  $H_3O^+$  ions was possible and less TiOH groups were formed. Subsequently, the combination with  $Ca^{2+}$  and  $HPO_4^{2-}$  ions and the deposition of a hydroxyapatite layer was inhibited.

## CONCLUSIONS

Alkali-treated titanium surfaces showed to induce apatite formation due to their sodium titanate layer. All heat treatments under air, argon flow or vacuum negatively affected the *in vitro* bioactivity. The thermal decomposition of the dense sodium titanate basis near

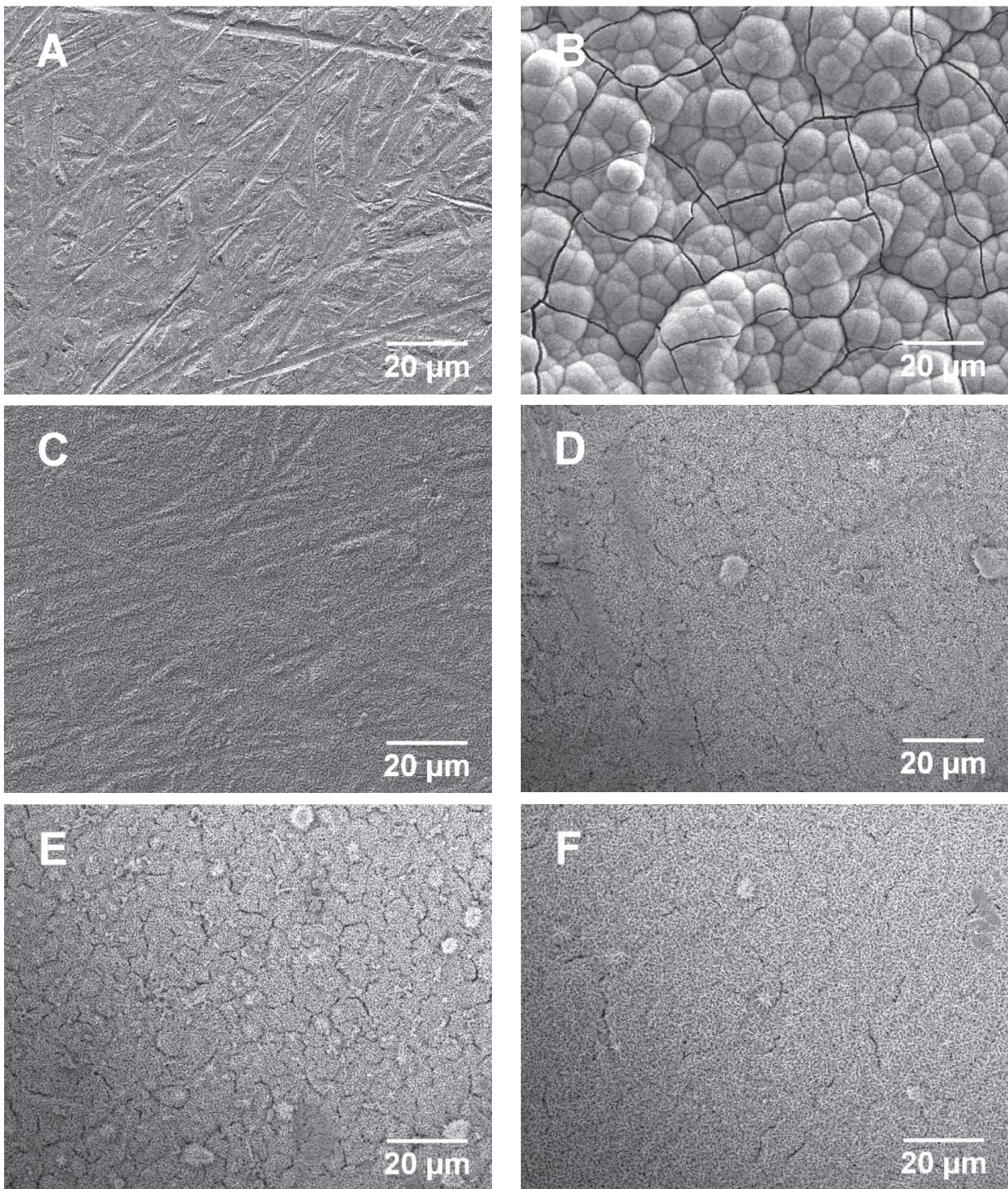


Figure 4. FESEM micrographs of alkali- and heat-treated surfaces after 7 days of immersion in SBF.

the interface with the titanium substrate into  $Ti_yO_z$  and sublimated  $Na_2O$  seemed to be detrimental, as confirmed by FESEM, TF-XRD, Raman and GDOES analysis. After all heat treatments, less exchangeable sodium ions remained available. This indicates that the ion exchange capacity of the sodium titanate layer is of high importance for *in vitro* bioactivity.

#### Acknowledgements

*V.M. is a postdoctoral fellow and E.V. a research assistant of the Fund for Scientific Research (FWO). The authors acknowledge Hong Chen, Raymond Kemps, Myrjam Mertens, Michel Schoeters, Dirk Vanhoyweghen and Roumen Vitchev from VITO's Centre for Materials*

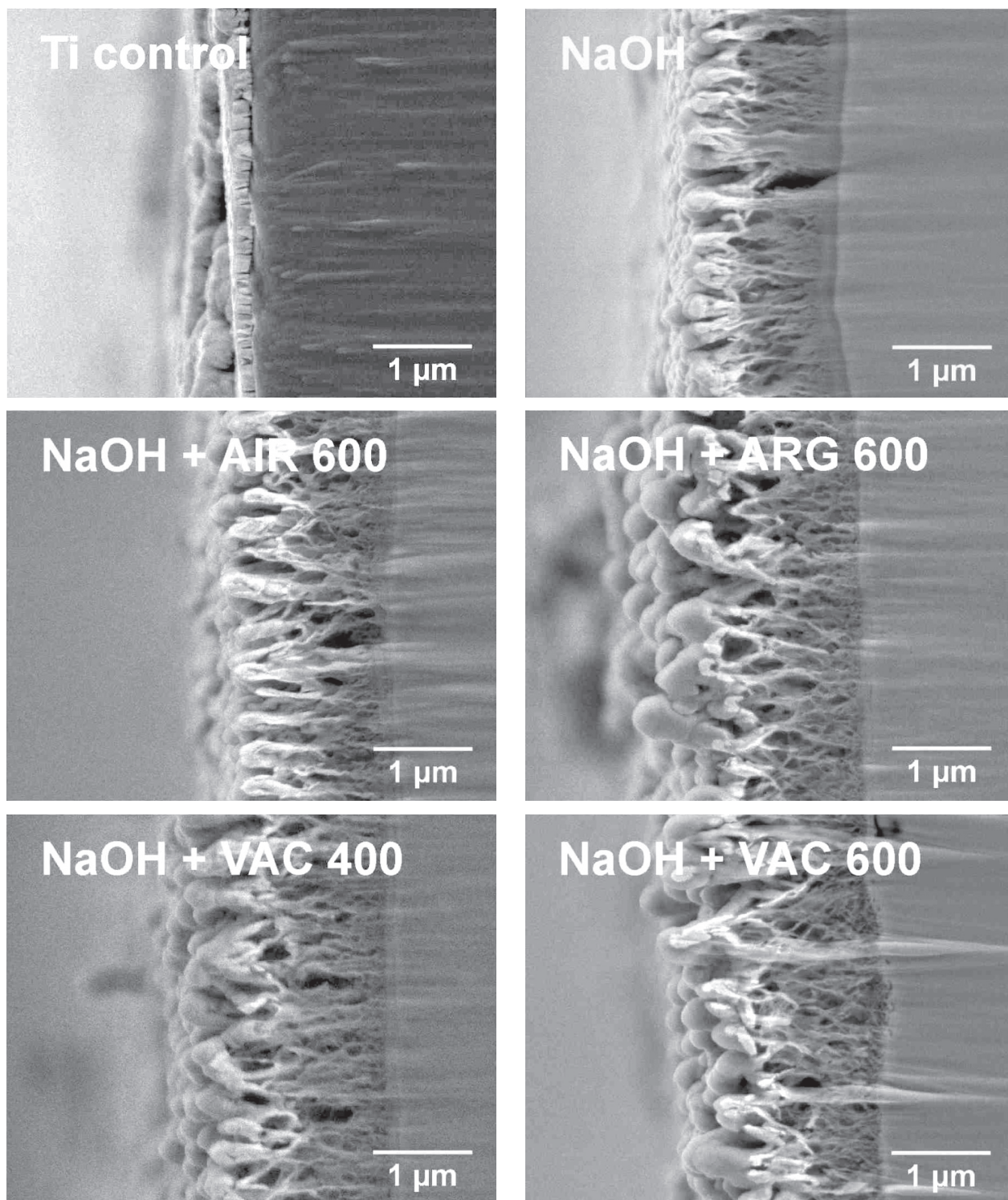


Figure 5. Cross section FESEM micrographs of alkali- and heat-treated samples.

*Advice and Analysis (CMA<sup>2</sup>) for the sample preparation and contact angle, FESEM, TF-XRD, XPS and GDOES measurements.*

References

1. Kim H. M., Miyaji F., Kokubo T., Nakamura T.: *J. Biomed. Mater. Res.* 32, 409 (1996).
2. Liang F. H., Zhou L., Wang K. G.: *Surf. Coat. Technol.* 165, 133 (2003).
3. Lin F. H., Hsu Y. S., Lin S. H., Chen T. M.: *Mater. Chem. Phys.* 87, 24 (2004).
4. Aparicio C., Manero J. M., Conde F., Pegueroles M., Planell J. A., Vallet-Regi M., Gil F. J.: *J. Biomed. Mater. Res. Part A* 82A, 521 (2007).
5. Wang X. J., Li Y. C., Lin J. G., Hodgson P. D., Wen C. E.: *J. Mater. Res.* 23, 1682 (2008).
6. Nishiguchi S., Nakamura T., Kobayashi M., Kim H. M., Miyaji F., Kokubo T.: *Biomaterials* 20, 491 (1999).
7. Nishiguchi S., Kato H., Fujita H., Kim H. M., Miyaji F., Kokubo T., Nakamura T.: *J. Biomed. Mater. Res.* 48, 689 (1999).
8. Nishiguchi S., Kato H., Fujita H., Oka M., Kim H. M., Kokubo T., Nakamura T.: *Biomaterials* 22, 2525 (2001).
9. Nishiguchi S., Fujibayashi S., Kim H.M., Kokubo T., Nakamura T.: *J. Biomed. Mater. Res. Part A* 67A, 26 (2003).
10. Kim H. M., Miyaji F., Kokubo T., Nakamura T.: *J. Mater. Sci.-Mater. Med.* 8, 341 (1997).
11. Chen Y.K., Zheng X. B., Ji H., Ding C. X.: *Surf. Coat. Technol.* 202, 494 (2007).
12. Wei D. Q., Zhou Y., Wang Y. M., Jia D. C.: *Thin Solid Films* 516, 6413 (2008).
13. Becker I., Hofmann I., Muller F. A.: *J. Eur. Ceram. Soc.* 27, 4547 (2007).
14. Kokubo T., Takadama H.: *Biomaterials* 27, 2907 (2006).
15. Braga F. J. C., Marques R. F. C., Filho E. D. A., Guastaldi A. C.: *Appl. Surf. Sci.* 253, 9203 (2007).
16. Glasser F. P., Marr J.: *J. Am. Ceram. Soc.* 62, 42 (1979).
17. Kasuga T., Hiramatsu M., Hoson A., Sekino T., Niihara K.: *Adv. Mater.* 11, 1307 (1999).
18. Menzel R., Peiro A. M., Durrant J. R., Shaffer M. S. P.: *Chem. Mat.* 18, 6059 (2006).
19. Qamar M., Yoon C. R., Oh H. J., Kim D. H., Jho J. H., Lee K. S., Lee W. J., Lee H. G., Kim S. J.: *Nanotechnology* 17, 5922 (2006).
20. Kasuga T., Hiramatsu M., Hoson A., Sekino T., Niihara K.: *Langmuir* 14, 3160 (1998).
21. Morgado E., de Abreu M. A. S., Pravia O. R. C., Marinkovic B. A., Jardim P. M., Rizzo F. C., Araujo A. S.: *Solid State Sci.* 8, 888 (2006).
22. Papp S., Korosi L., Meynen V., Cool P., Vansant E. F., Dekany I.: *J. Solid State Chem.* 178, 1614 (2005).
23. Jonasova L., Muller F. A., Helebrant A., Strnad J., Greil P.: *Biomaterials* 23, 3095 (2002).
24. Takemoto M., Fujibayashi S., Neo M., Suzuki J., Matsushita T., Kokubo T., Nakamura T.: *Biomaterials* 27, 2682 (2006).